SIPP1, a novel pre-mRNA splicing factor and interactor of protein phosphatase-1

Miriam LLORIAN*, Monique BEULLENS†, Isabel ANDRÉS*, Jose-Miguel ORTIZ* and Mathieu BOLLEN†[1]

*Departamento de Biologia Molecular, Facultad de Medicina, Universidad de Cantabria, Unidad Asociada al CIB-CSIC, 39011 Santander, Spain, and †Division of Biochemistry, Faculty of Medicine, Catholic University of Leuven, Herestraat 49, B-3000 Leuven, Belgium

We have identified a polypeptide that was already known to interact with polyglutamine-tract-binding protein (PQBP)-1/Npw38 as a novel splicing factor and interactor of protein phosphatase-1, hence the name SIPP1 for splicing factor that interacts with PQBP-1 and PP1 (protein phosphotase 1). SIPP1 was inhibitory to PP1, and its inhibitory potency was increased by phosphorylation with protein kinase CK1. Two-hybrid and co-sedimentation analysis revealed that SIPP1 has two distinct PP1-binding domains and that the binding of SIPP1 with PP1 involves a RVXF (Arg-Val-Xaa-Phe) motif, which functions as a PP1-binding sequence in most interactors of PP1. Enhanced-green-fluorescent-protein-tagged SIPP1 was targeted exclusively to the nucleus and was enriched in the nuclear speckles, which represent storage/assembly sites of splicing factors. We have mapped a nuclear localization signal in the N-terminus of SIPP1, while the proline-rich C-terminal domain appeared to be required for its subnuclear targeting to the speckles. Finally, we found that SIPP1 is also a component of the spliceosomes and that a SIPP1-fragment inhibits splicing catalysis by nuclear extracts independent of its ability to interact with PP1.

Key words: dephosphorylation, polyglutamine tract, protein phosphatase-1 (PP1), SIPP1, spliceosome, splicing.

INTRODUCTION

Protein phosphatase-1 (PP1) is a ubiquitous protein serine/threonine phosphatase that functions in a variety of processes, including intermediate metabolism, protein synthesis, cell-cycle progression and intracellular transport [1–4]. Mammalian genomes contain three genes that altogether encode four isoforms of PP1, namely PP1α, PP1β/δ and the splice variants PP1γ1 and PP1γ2. These isoforms have a nearly identical catalytic core and substrate specificity, but, for reasons that are not yet understood, they interact *in vivo* with distinct, albeit overlapping, sets of proteins. The protein interactors target PP1 to specific cellular compartments or substrates and also function as substrate specifiers. Some interactors, mostly protein kinases, are themselves substrates for associated PP1. The regulation of PP1 by hormones, growth factors and metabolites is largely mediated by the phosphorylation or allosteric regulation of its interactors, resulting in an altered activity, substrate specificity and/or affinity of associated PP1.

More than 60 mammalian genes are already known to encode interactors of PP1 [1–4]. The available data suggest that these interactors bind to PP1 via multiple short-sequence motifs. For example, most of the interactors contain a PP1-binding motif of the RVXF (Arg-Val-Xaa-Phe) type, which is actually a degenerate four- or five-residue motif that conforms to the consensus sequence [R/K]-X_{0-1}-[V/I]-{P}-[F/W], where X is any residue and {P} is any residue except proline [5–7]. Binding of the RVXF motif to a hydrophobic pocket of PP1 that is remote from the catalytic site in itself does not have major effects on the activity and conformation of the phosphatase, but has been proposed to have a 'proximity' effect and to promote the interaction with PP1 of secondary, lower-affinity binding sites that bring about interactor-specific effects on the activity and substrate specificity of PP1. Since PP1 interactors can also share binding sites other than the RVXF motif, this has led us to propose that PP1 is subject to a combinatorial control, implying that the activity and substrate specificity of PP1 is determined by the 'combination' of binding sites that are occupied by the interactors [1]. This combinatorial control model can also explain how a huge variety of interactors can have specific effects on PP1, in spite of the limited number of distinct binding sites on PP1.

Various approaches have been used to identify novel regulators of PP1. Initially, new interactors were mainly found by the characterization of newly purified PP1 holoenzymes [8–11]. More recently, MS and tools of bioinformatics have been instrumental in establishing the PP1 interactome [12–13]. However, by far the most PP1 interactors have been identified by yeast two-hybrid screenings with PP1 as bait [14–17]. In the present paper, we report on the identification by yeast two-hybrid screening of a novel interactor of PP1, termed SIPP1 [for splicing factor that interacts with polyglutamine-tract-binding protein (PQBP-1) and PP1], a protein that was already known to bind to PQBP-1/Npw38 [18] and also to SH3 (Src homology 3)-domains *in vitro* [19]. We have mapped the SIPP1–PP1 interaction sites as well as the sequences that mediate the targeting of SIPP1 to the nucleus and to nuclear storage sites for splicing factors. Finally, we show that SIPP1 is a component of the spliceosomes and that SIPP1 fragments block pre-mRNA splicing catalysis in nuclear extracts.

EXPERIMENTAL

Materials

The catalytic subunit of PP1 was prepared from rabbit skeletal muscle [20]. Polyclonal antibodies against a synthetic peptide

Abbreviations used: EGFP, enhanced green fluorescent protein; GADD34, growth arrest and DNA-damage-inducible protein; GST, glutathione S-transferase; HA, haemagglutinin; NIPP1, nuclear inhibitor of PP1; NLS, nuclear localization signal; PP1, protein phosphatase-1; PQBP-1, polyglutamine-tract-binding protein; SH3, Src homology 3; SIPP1, splicing factor that interacts with PQBP-1 and PP1; TBS, Tris-buffered saline.

[1] To whom correspondence should be addressed (e-mail Mathieu.Bollen@med.kuleuven.ac.be).

comprising the 15 C-terminal residues of SIPP1 (DDVYEAFM-KEMEGLL), and coupled to keyhole-limpet haemocyanin, were generated in rabbits. The antibodies were affinity-purified on the BSA-coupled peptides linked to CNBr-activated Sepharose 4B. Anti-EGFP (enhanced green fluorescent protein) and anti-GAL4 (DNA-binding domain) antibodies and anti-rabbit secondary antibodies were purchased from Santa Cruz Biotechnology (Santa Cruz, CA, U.S.A.). Anti-haemagglutinin (HA) antibodies were obtained from Sigma–Aldrich. Anti-mouse secondary antibodies and restriction enzymes were from Amersham Biosciences. *Pfu* DNA polymerase was purchased from Stratagene. Alanine-scanning mutants of *Glc7* were described previously [21] and were a gift from Dr K. Tatchell (Department of Biochemistry and Molecular Biology, Louisiana State University Medical Center, Shreveport, LA, U.S.A.).

Yeast two-hybrid assays

A mouse embryo MATCHMAKER cDNA library (NIH-3T3), subcloned in the pACT2 vector in frame with the GAL4 activation domain, was obtained from Clontech. PP1β/δ, PP1γ1 and PP1γ2, and mutants/fragments of these phosphatases were subcloned in-frame with the GAL4 DNA-binding domain in the pODB8 vector, and Glc7 and PpZ1 were subcloned into pAS2 vector [22]. The HF7C or Y187 reporter strains were transformed using the lithium acetate transformation protocol, as described in the Clontech Yeast Protocols Handbook (http://www.bdbiosciences.com/clontech/techinfo/manuals/PDF/PT3024-1.pdf). β-Galactosidase activity was detected in colony-lift filter assays with X-gal (5-bromo-4-chloroindol-3-yl β-D-galactopyranosidase) as a substrate, as described in the Clontech Yeast Protocols Handbook. Blue colouring was monitored visually. For quantitative assays, Y187 transformants were grown overnight in liquid medium and the β-galactosidase activity was detected with *o*-nitrophenyl β-D-galactopyranoside as a substrate. The expression of the constructs in yeast lysates was verified by Western blot analysis with anti-GAL4 or anti-HA antibodies.

Expression vectors and DNA constructs

For the mapping of the PP1-binding domains of SIPP1 by yeast two-hybrid analysis, full-length SIPP1 and truncated versions comprising amino acids 45–641, 164–258 and 253–641 were PCR-amplified with appropriate primers, with tails containing pACT2-compatible restriction sites, and the amplified fragments were subcloned in frame with the GAL4 activation domain. The same truncated versions of SIPP1 as well as SIPP1-(180–372), SIPP1-(359–641) and SIPP1-(253–372) were also subcloned into the pGEX3X vector to obtain GST (glutathione S-transferase)-fusion proteins. Point mutations were introduced using the QuikChange™ site-directed mutagenesis kit (Stratagene). For subcellular localization experiments, SIPP1-(1–641), SIPP1-(1–45), SIPP1-(45–641), SIPP1-(1–372), SIPP1-(358–641), SIPP1-(1–641)-K31A/K32A/K34A/K35A (Lys → Ala mutations) and SIPP1-(1–641)-V219A/F221A/V308A/F310A (Val/Phe → Ala mutations) were amplified by PCR and subcloned in-frame with EGFP in the pEGFP-C1 plasmid. All constructs and mutants were verified by DNA sequencing.

Preparation of recombinant proteins

Escherichia coli BL21 cells transformed with different pGEX3X constructs were grown at 37 °C. The expression of the proteins was induced by the addition to the culture of 1 mM IPTG (isopropyl β-D-thiogalactoside). After growth at 30 °C for 2–3 h, the bacteria were collected by centrifugation at 5000 ***g*** for 10 min and stored at − 80 °C. Frozen pellets were resuspended in a solution containing 50 mM Tris/HCl, pH 7.5, 0.3 M NaCl, 1 mM dithiothreitol, 0.1 % (w/v) 2-mercaptoethanol, 0.5 % (v/v) Triton X-100, 0.5 mM PMSF, 0.5 mM benzamidine and 0.5 μM leupeptin. Cell lysis was enhanced by brief sonication. After centrifugation at 20 000 ***g*** for 20 min, the supernatant was diluted with 1 vol. of the same buffer lacking NaCl, and applied to 2 ml of glutathione–agarose. The retained GST-fusion proteins were eluted with 0.1 M Tris/HCl at pH 8 and 10 mM reduced glutathione. The purified proteins were dialysed in 50 mM Tris/HCl, pH 7.5, and 150 mM NaCl.

Cell culture

COS-1 cells, HeLa cells and HEK-293T cells were grown in Dulbecco's modified Eagle's medium supplemented with 10 % (v/v) foetal calf serum on 10-cm-diameter plates or on sterile Lab-Tek™ Chambered Coverglass (Nunc). At 1 day after seeding, COS-1 and HeLa cells were transfected with 0.1–2 μg/ml plasmid DNA, using the FuGene™ 6 transfection reagent (Roche Diagnostics), according to the manufacturer's protocol. HEK-293T cells were transfected using the calcium phosphate protocol [23]. COS-1 or HEK-293T cells were harvested in a lysis buffer containing 20 mM Tris/HCl, pH 8.0, 50 mM NaCl, 1 mM EDTA, 0.5 % (w/v) Nonidet P40, 0.5 mM PMSF, 0.5 mM benzamidine and 0.5 μM leupeptin. After incubation for 30 min on ice, the homogenates were centrifuged for 10 min at 13 000 **g**. The supernatant is referred to as the cell lysate. For (co-)immunoprecipitation experiments, cells were harvested in a solution containing 20 mM Tris/HCl, pH 7.5, 0.3 M NaCl, 0.5 % (v/v) Triton X-100, 1 mM dithiothreitol, 0.5 mM PMSF, 0.5 mM benzamidine and 0.5 μM leupeptin, and cell lysates were prepared as indicated above. The subcellular localization of EGFP-tagged SIPP1 (fragments) was studied by fluorescence microscopy 24–48 h after transfection of HeLa cells.

GST pull-down assays

GST (270 nmol) or the indicated GST–SIPP1 mutants were incubated for 1 h at 4 °C with 50 μl of glutathione–agarose beads in 20 mM Tris/HCl, pH 7.4, 150 mM NaCl and 1 mM dithiothreitol. The beads were washed twice with 500 μl of buffer and resuspended either in 50 μl of the same buffer, supplemented with 1 mg/ml BSA and 15 nM PP1 purified from rabbit skeletal muscle (see Figures 2B and 3), or in lysates from cells that had been transfected with HA-tagged PP1γ2 (see Figure 2A). After incubation for 1 h at 4 °C, the beads were washed three times in 500 μl of Tris-buffered saline (TBS) and once more in 50 mM glycylglycine, pH 7.4, 0.5 mM dithiothreitol and 5 mM 2-mercaptoethanol. The co-precipitation of PP1 with the GST–SIPP1 fusion proteins was evaluated by the assay of the trypsin-revealed phosphorylase phosphatase activity [24] or by Western blotting with anti-HA antibodies. For peptide competition assays (see Figure 3C below), PP1 associated with glutathione–agarose bound GST–SIPP1-(180–372) was incubated for 30 min at 4 °C with 500 μM NIPP1 (nuclear inhibitor of PP1)-(197–206) or NIPP1-(197–206)-V201A/F203A. Subsequently, PP1 released in the supernatant was quantified by the assay of phosphorylase phosphatase after trypsinolysis and the activity was expressed as a percentage of the total activity that was associated with the beads before incubation with the peptides.

Immunological procedures

For Western blot analysis, the samples were subjected to (Tricine/) SDS/PAGE, blotted on to PVDF membranes and incubated for 2 h

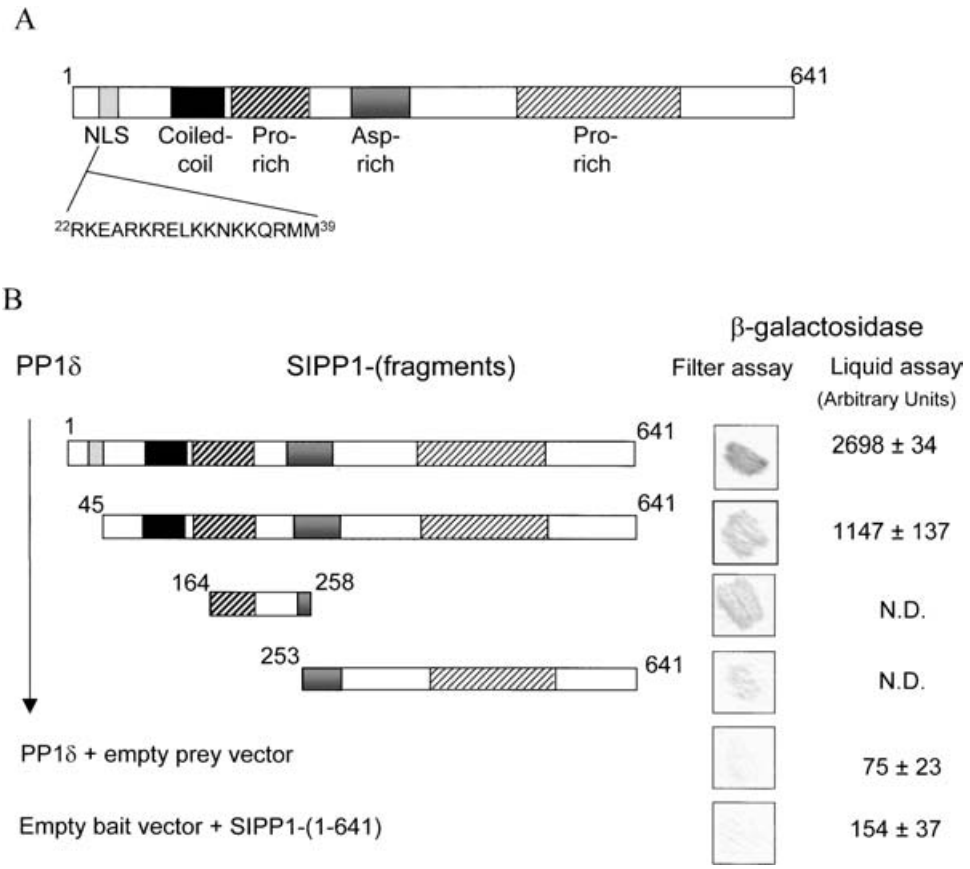

Figure 1 SIPP1 interacts with PP1 in two-hybrid assays

(**A**) Domain structure of SIPP1, as predicted by the ISREC motif scan (http://hits.isb-sib.ch/cgi-bin/PFSCAN). (**B**) Interaction between PP1$\delta\gamma$ and SIPP1 (fragments), as determined by yeast two-hybrid assays. The Figure shows β-galactosidase activities from both colony-lift filter assays (yeast strain HF7C) and liquid assays (yeast strain Y187). The liquid assay data are represented as means $\pm$ S.E.M. for six observations. ND, not determined for lack of expression of the prey protein.

at 4 °C with primary antibodies, i.e. antibodies against EGFP, the HA epitope or SIPP1. Subsequently, the blots were incubated with peroxidase-labelled secondary antibodies (45 min at 4 °C) and the retained secondary antibodies were visualized by enhanced chemiluminescence (ECL®; Amersham Biosciences). Immunoprecipitations were carried out with cell lysates from three 10-cm-diameter plates. After addition of anti-SIPP1 antibodies, the samples were incubated for 1 h at 4 °C. Subsequently, 50 μl of Protein A–TSK® (Affiland, Liège, Belgium) was added and the mixture was incubated for 30 min at 4 °C in a rotary shaker at 1400 rev./min. The beads were washed three times with TBS and then once more with 50 mM glycylglycine, pH 7.4, 0.5 mM dithiothreitol and 5 mM 2-mercaptoethanol. PP1 in the immunoprecipitates was quantified by the assay of spontaneous and trypsin-revealed phosphorylase phosphatase activities or by Western blot analysis with anti-EGFP or anti-HA antibodies.

Northern blot

A mouse adult tissue RNA blot from Seegene® (Seoul, South Korea) was hybridized with a probe derived from the SIPP1 cDNA (nucleotides 292–514). Probes were labelled using the Ready-To-Go™ DNA labelling Kit (-dCTP) (Amersham Biosciences) to a specific radioactivity of approx. 10^9 c.p.m./μg. Hydridizations were performed at 65 °C for 6 h in the ExpressHyb™ hybridization solution from Clontech, supplemented with 100 μg/ml of denaturated salmon sperm DNA. Subsequently, the membranes were washed twice with 0.3 M NaCl/0.03 M citrate and 0.1 % (w/v) SDS at 60 °C for 20 min, and twice with 0.15 M NaCl/0.015 M citrate and 0.1 % (w/v) SDS under the same conditions. The bands were visualized by autoradiography.

Splicing assays

A capped β-globin pre-mRNA fragment comprising exon 1 through the *Bam*HI site in exon 2, was synthesized in the presence of [α-^{32}P]GTP. This primary transcript was used as substrate for splicing in HeLa cell nuclear extracts [25].

RESULTS

SIPP1 is a novel interactor of PP1

Using PP1γ2 and PP1δ as baits in a yeast two-hybrid screening of a mouse embryo cDNA library, we identified a prey protein that has been described previously as an interactor of the nuclear protein PQBP-1/Npw38 [18], and also as an SH3-domain-binding protein *in vitro* [19]. Since we have found that this novel PP1 interactor functions as a pre-mRNA splicing factor (see below), we will refer further to this protein as SIPP1. SIPP1 (641 residues) is a modular protein with a putative bipartite nuclear localization signal (NLS), a coiled-coil region, two proline-rich regions and an aspartate-rich region (Figure 1A).

The two prey clones that we isolated both encoded a N-terminally nicked polypeptide, namely SIPP1-(45–641) (Figure 1B). However, full-length SIPP1 interacted even better with PP1δ in the two-hybrid system. Using smaller SIPP1 fragments, we were able to identify two PP1-interacting regions, one comprising residues 164–258 and the other comprising residues 253–641. A more detailed mapping of the PP1-binding sites with the two-hybrid approach was not possible, since smaller SIPP1 fragments were not expressed well in yeast strain HF7C (results not shown). We have also performed two-hybrid assays in another yeast strain (Y187), which moreover enabled us to do more quantitative (liquid) assays. Although the latter experiments confirmed the SIPP1–PP1 interaction (Figure 1B), they did not provide additional data on the PP1-interaction sites, since only full-length SIPP1 and SIPP1-(45–641) were expressed in this yeast strain (results not shown).

To gain more insight into the regions of SIPP1 that interact with PP1, we have generated SIPP1 fragments as GST-fusion proteins in bacteria, and have used the purified fusions for GST pull-down assays of HA-tagged PP1γ2 that was transiently expressed in HEK-293 cells. The data confirmed the two-hybrid assays in that GST-tagged SIPP1-(164–258) and SIPP1-(253–641) pulled down HA–PP1γ2 from HEK-293 cell lysates, as detected by immunoblotting (Figure 2A). In addition, SIPP1-(180–372) and SIPP1-(253–372) also clearly interacted with PP1 in the GST pull-down assays, whereas SIPP1-(359–641) did not, thus enabling us to map in more detail the second PP1 interaction site. The GST–SIPP1 fusions, coupled to glutathione–agarose, were also used to measure their ability to interact with the catalytic subunit of PP1 that was purified from rabbit skeletal muscle (Figure 2B). The relative affinities were very similar to that found for PP1 in cell lysates (Figure 2A), showing that SIPP1 binds directly to PP1.

The above data indicated that SIPP1 has at least two PP1-interaction sites: one in residues 164–258 and a second in residues 253–372. Most interactors of PP1 contain a so-called RVXF motif that mediates binding to a hydrophobic channel of PP1 that is remote from the catalytic site (see the Introduction). SIPP1-(164–258) contains a consensus RVXF sequence, namely $R^{217}KVGF^{221}$. SIPP1-(253–372) also harbours a RVXF-like sequence, $L^{306}SVRF^{310}$, which, however, lacks an N-terminal basic residue. The combined V219A and F221A mutations decreased the binding of GST–SIPP1-(164–258) to PP1 in pull-down assays (Figure 3A). Likewise, the V308A and F310A mutations nearly abolished the interaction of SIPP1-(253–372) with PP1. These double mutations did not affect the binding of the larger SIPP1-(180–372) to PP1, but a combination of all four mutations yielded a protein that barely interacted with PP1. These data provide additional evidence for the existence of at least two distinct PP1-binding sites in SIPP1.

We have subsequently explored whether the mutation of these two PP1-binding sites also abolished the binding of full-length SIPP1 to PP1. Since GST–SIPP1 could not be expressed in bacteria, we have co-expressed HA-tagged PP1γ2 and either EGFP-tagged SIPP1-(1–641) or EGFP-tagged SIPP1-(1–641)-V219A/F221A/V308A/F310A in COS-1 cells. In accordance with the GST pull-down experiments (Figure 3A), we found that HA–PP1γ2 co-immunoprecipitated with EGFP–SIPP1-(1–641), but not with the EGFP–SIPP1-(1–641) mutant, as detected by Western blot analysis, as well as phosphorylase phosphatase assays (Figure 3B).

To examine further whether or not SIPP1 contains a functional RVXF motif, we performed competition studies with a synthetic peptide that comprises residues 197–206 of the PP1-interactor NIPP1 and that includes the established RVXF motif of NIPP1 [7]. In Figure 3(C), it is shown that this peptide disrupted the interaction between PP1 and GST–SIPP1-(180–372), whereas a peptide with a mutated RVXF motif, i.e. NIPP1-(197–206)-V201A/F203A, had no effect. These data provide additional evidence for an essential role of an RVXF motif in the binding to PP1 (see also the Discussion).

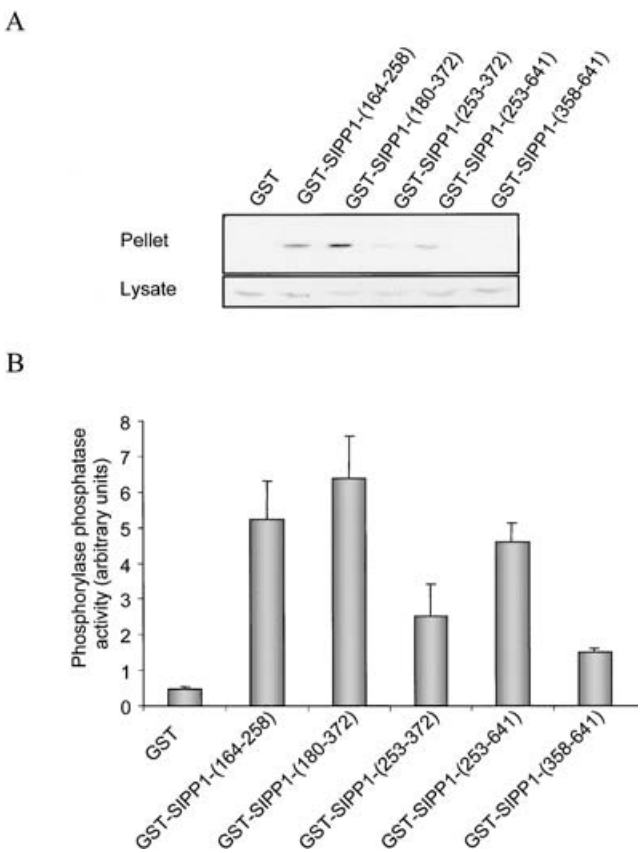

Figure 2 Co-precipitation of SIPP1 and PP1

(**A**) Pull-down of HA-tagged PP1γ2 with GST-tagged SIPP1 fragments. Equimolar amounts of GST and GST-tagged fusions of SIPP1 fragments were bound to glutathione–agarose beads. The washed beads were incubated with lysates from HEK-293T cells that had been transfected with HA–PP1γ2. The retained HA–PP1γ2 was quantified by Western blot analysis with anti-HA antibodies. (**B**) Recombinant GST-tagged SIPP1 fusions, coupled to glutathione–agarose, were incubated with the catalytic subunit of PP1 purified from rabbit skeletal muscle. The retained phosphatase activities were quantified by the assay of phosphorylase phosphatase activities after the release of PP1 from the beads by a pre-incubation with trypsin. The results are means $\pm$ S.E.M. for three phosphatase assays.

Mapping of SIPP1-binding sites of PP1

Mammalian genomes harbour three genes that altogether encode four isoforms of PP1 (see the Introduction). To examine whether or not the interaction of SIPP1 with PP1 was isoform-dependent, full-length SIPP1 and PP1α, PP1β/δ or PP1γ1 were transiently expressed in COS-1 cells as fusions with EGFP (Figure 4A). Subsequently, EGFP–SIPP1 was immunoprecipitated from the cell lysates with antibodies directed against the C-terminus of SIPP1. We found that all three PP1 isoforms could be immunoprecipitated with anti-SIPP1 antibodies, as detected both by Western blot analysis (Figure 4B) and by protein phosphatase activity assays (results not shown). PP1α was clearly precipitated less well, which may be explained by a somewhat lower expression level of this isoform (Figure 4A).

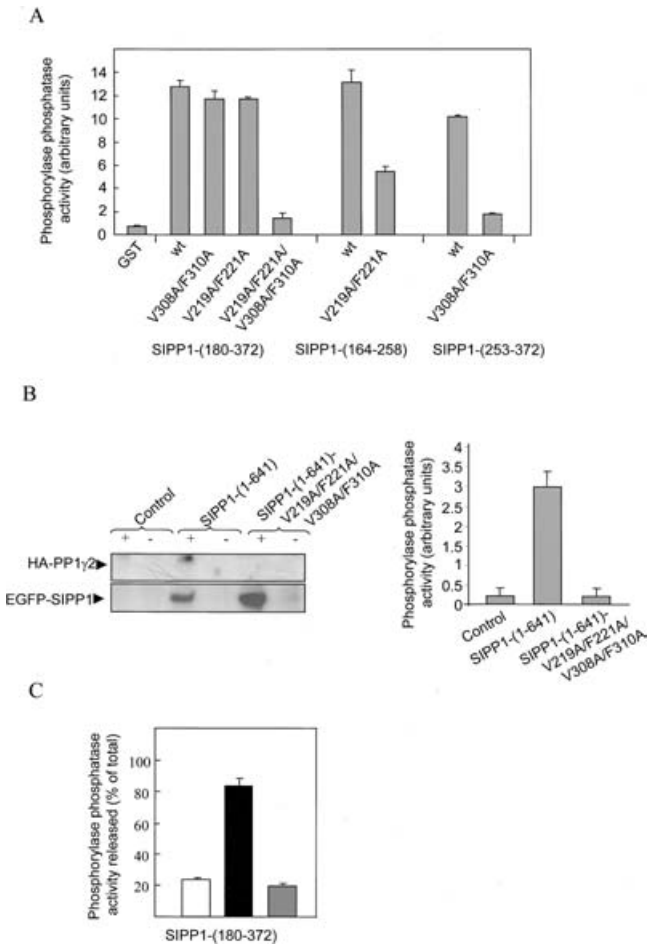

Figure 3 SIPP1 contains a functional RVXF motif

(**A**) The interaction of PP1 from rabbit skeletal muscle with GST-fusions of the indicated SIPP1 mutants was analysed by GST pull-down assays and was quantified by the assay of the trypsin-revealed phosphorylase phosphatase activity that was associated with the glutathione–agarose beads. (**B**) EGFP–SIPP1-(1–641) and EGFP–SIPP1-(1–641)-V219A/F221A/V308A/F310A were transfected into COS-1 cells. SIPP1 was inmunoprecipitated with anti-EGFP antibodies, and the interaction between PP1 and SIPP1 was quantified by measuring the trypsin-revealed phosphorylase phosphatase activities that were associated with the immunocomplexes (right-hand panel). The results are means ± S.E.M. for three assays. The control refers to mock-transfected cells. The left-hand panel shows the level of HA–PP1γ2 and EGFP–SIPP1 in the immunoprecipitates using anti-HA and anti-EGFP antibodies. The immunoprecipitates were obtained with (+) and without (−) primary anti-EGFP antibodies. (**C**) GST-tagged SIPP1-(180–372) bound to glutathione–agarose and saturated with purified PP1 was incubated for 30 min at 4 °C with buffer (white bar), 500 μM NIPP1-(197–206) containing a functional RVXF motif (black bar) or 500 μM NIPP1-(197–206)-V201A/F203A, i.e. with a mutated RVXF motif (grey bar). Subsequently, the beads were sedimented and the trypsin-revealed phosphorylase phosphatase activity was measured in the supernatant. The released activities were expressed as a percentage of the total activity that was associated with the beads. The results are means ± S.E.M. for three different experiments.

The lack of isoform specificity of the SIPP1–PP1 interaction was confirmed by yeast two-hybrid assays using PP1δ, PP1γ1 and PP1γ2 as bait (results not shown). These assays revealed further that SIPP1 also interacts with Glc7, the PP1 orthologue of *Saccharomyces cerevisiae* and with the catalytic domain of Ppz1, a PP1-like enzyme from *S. cerevisiae* that is nearly 70 % identical with the conserved portion of mammalian PP1 isoforms [13].

RVXF motifs are known to bind to a hydrophobic channel of PP1 that is formed by the edges of two β-sheets [5]. PP1δ1-Δ286–323, which is truncated just before the last β-strand (β14) that contributes half of the residues that line the RVXF-binding channel, did not interact with SIPP1 in two-hybrid assays [267 ± 8 units of β-galactosidase compared with 2697 ± 334 units for the wild-type PP1δ and 254 ± 20 units for the empty bait vector, ($n = 6$)], confirming that SIPP1 interacts via a RVXF motif. We have shown previously that this truncation mutant of PP1γ1 still binds to Sds22, which does not contain a RVXF motif [13]. On the other hand, Sds22 was shown to interact with the α4/α5/α6 triangle of PP1, and two point mutants of the α6-helix, PP1γ1-K147A and PP1γ1-K150A, did not interact with Sds22. The latter two mutants still interacted normally with SIPP1 in two-hybrid assays (results not shown), indicating that SIPP1 does not bind to the α6 helix of PP1.

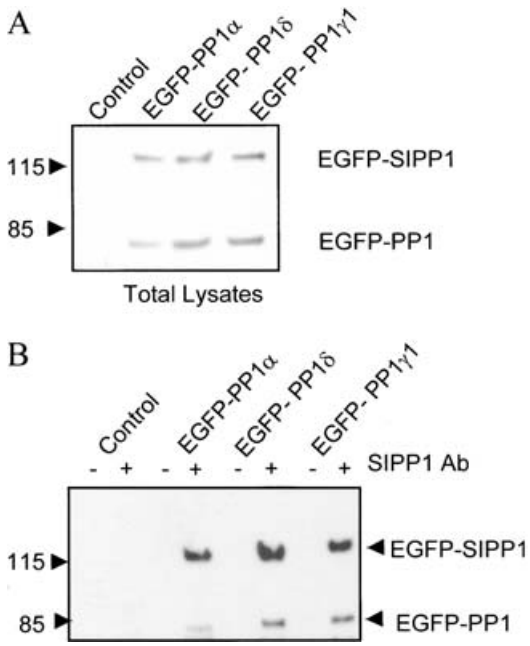

Figure 4 The interaction of SIPP1 with PP1 is isoform-independent

(**A**) COS-1 cells were transfected with both EGFP-tagged SIPP1 and the indicated EGFP-tagged PP1 isoforms. The expression of the tagged proteins in cell lysates was detected with anti-EGFP antibodies. (**B**) SIPP1 was immunoprecipitated from the lysates with antibodies against SIPP1 and the immunoprecipitated EGFP–SIPP1, and co-precipitated EGFP–PP1 isoforms were visualized by Western blotting with antibodies against EGFP.

To map further additional surface areas of PP1 that are involved in the interaction with SIPP1, we have used a panel of 'charged-to-alanine' mutant alleles of Glc7 in two-hybrid assays [21]. The expression of all mutants was verified (Figure 5B). Three products of the tested mutant alleles, *glc7-126*, *glc7-127* and *glc-128*, showed no interaction with full-length SIPP1 and one mutant allele, *glc7-136*, showed a reduced interaction (Figure 5A). These data suggest that mutation of (some) residues close to the catalytic site, as in *glc7-126*, is detrimental to the binding of SIPP1. Both residues that are mutated in *glc7-128* (Arg^{121} and Glu^{125}) and one of the two residues mutated in *glc7-127* (Lys^{110}) are expected to be buried, based on the known crystal structure of mammalian PP1 [26,27], implying that these residues cannot interact directly with SIPP1.

SIPP1 is a regulator of PP1

We have also investigated whether or not SIPP1 interferes with the protein phosphatase activity of PP1. Following the expression of EGFP–SIPP1 and HA-tagged PP1γ2 in COS-1 cells, SIPP1 was immunoprecipitated from the cell lysates and the immunoprecipitates were analysed for protein phosphatase activity,

A

Allele	Mutations	SIPP1-(1-641)
GLC7-wt	-	1365 ± 248
glc7-101	E53A/E55A	1831 ± 67
glc7-102	E76A	1547 ± 87
glc7-106	E217A/D219A	1921 ± 268
glc7-108	E255A	1742 ± 328
glc7-109	K259A/R260A	2938 ± 402
glc7-111	D285A/E286A	2097 ± 382
glc7-121	D7A/D9A	1732 ± 223
glc7-122	D13A/R14A/E17A	3072 ± 468
glc7-126	D94A/ R95A/ K97A	220 ± 44
glc7-127	K110A/K112A	160 ± 24
glc7-128	R121A/E125A	154 ± 14
glc7-132	D165A/E166A/K167A	2222 ± 292
glc7-133	R186A/R187A/R190A/Q298K	3231 ± 189
glc7-134	D193A/D196A	2051 ± 485
glc7-136	D229A/R233A	799 ± 83
Empty bait vector	-	254 ± 20

B

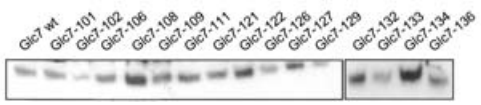

Figure 5 Interaction of SIPP1 with 'charged-to-alanine' mutants of the yeast PP1 orthologue Glc7

(**A**) The interaction between SIPP1-(1–641) and the indicated Glc7 mutants in liquid two-hybrid assays. The results are means (arbitrary units) ± S.E.M. for six observations. (**B**) Expression of all Glc7 mutants in the yeast extracts, as detected by Western blot analysis with antibodies against the GAL4 DNA-binding domain.

using glycogen phosphorylase *a* as substrate. In Figure 6(A), it is shown that the SIPP1 immunoprecipitates contained a barely detectable phosphorylase phosphatase activity (open bars). However, a large activity was revealed by trypsinolysis (solid bars), which is known to destroy most regulators of PP1 and to set free active catalytic subunit [25]. The latter activity was completely blocked by NIPP1, a specific inhibitor of PP1 (results not shown). EGFP–SIPP1-(180–372) also co-immunoprecipitated HA–PP1γ2 and the associated activity could also only be revealed by trypsinolysis.

The above data indicated that PP1 that is co-immunoprecipitated with SIPP1 or SIPP1-(180–372) from cell lysates is inactive. To explore whether this inhibition of PP1 is mediated by SIPP1 itself or by a third component, we have examined whether recombinant SIPP1-(180–372), which contains both PP1-interaction sites (Figures 1 and 2), affects PP1. SIPP1-(180–372) was indeed inhibitory to the phosphorylase phosphatase activity of PP1, but only at micromolar concentrations. Some regulators of PP1, such as Inhibitor-1 and CPI-17, are only inhibitory after phosphorylation [1,3,4]. Likewise, we found that SIPP1-(180–372) is an *in vitro* substrate of protein kinase CK1 and that the phosphorylation of SIPP1 is associated with a 10-fold increase of its inhibitory potency (Figure 6B). Yet, even after phosphorylation, SIPP1-(180–372) remained a poor inhibitor of PP1. This indicates that the inhibition of PP1 in the SIPP1-(180–372) immunoprecipitates is mediated by another polypeptide or that recombinant SIPP1-(180–372) does not have the proper conformation or post-translational modification (see the Discussion).

(Sub)cellular distribution of SIPP1

To obtain some initial information on the cellular processes that are affected by SIPP1, we have explored its tissue and subcellular distribution. Northern blot analysis revealed that SIPP1 is expressed in all tested mouse tissues, but its transcript was particularly abundant in testis (Figure 7A). The expression of SIPP1 in COS-1 and HeLa cells could also be visualized by immunofluorescence analysis using antibodies against the C-terminus (Figure 7B). In these cells, SIPP1 was mainly present in the nucleus, where it displayed a non-uniform, speckled distribution and appeared to be excluded from the nucleoli. However, a distinct pool of SIPP1 was associated with cytoskeletal elements in the cytoplasm. The latter findings are in accordance with the report that SIPP1 is associated with vimentin-containing intermediate filaments and co-localizes with splicing factors in the nuclear 'speckles' or splicing factor compartments [19].

We have subsequently mapped the determinants of the nuclear and subnuclear localization of SIPP1. For that reason, SIPP1 (fragments) were expressed as fusions with EGFP in HeLa cells. As expected, EGFP alone displayed a uniform cellular distribution (Figure 8A). In contrast, a fusion of EGFP and full-length SIPP1 showed a speckled nuclear distribution (Figure 8B), in accordance with the localization of endogenous SIPP1 (Figure 7B). However, EGFP–SIPP1 did not appear to be associated with cytoskeletal filaments, as was observed for endogenous SIPP1, which could indicate that the EGFP tag hampers the interaction with the cytoskeleton. Deletion of the C-terminal region, as in EGFP–SIPP1-(1–372), did not affect the nuclear localization, but abolished the speckled subnuclear distribution entirely (Figure 8C). These data suggest that the C-terminal domain, which comprises a proline-rich region, is involved in the targeting of SIPP1 to the splicing factor compartments. On the other hand, EGFP–SIPP1-(358–641) was nearly exclusively cytoplasmic (Figure 8D), indicating that the N-terminal half of SIPP1 harbours one or more NLSs. The ISREC motif scan (http://hits.isb-sib.ch/cgi-bin/PFSCAN) indeed predicts that residues 22–39 of SIPP1 comprise a bipartite nuclear localization sequences (Figure 1A). Moreover, a fusion of EGFP and the N-terminal 45 residues of SIPP1 was entirely nuclear (Figure 8E), whereas the N-terminal truncation of SIPP1, as in EGFP–SIPP1-(45–641), abolished its exclusive nuclear localization (compare Figures 8B and 8F). These data show that the N-terminal 45 residues of SIPP1 contain a functional NLS. In accordance with this interpretation, we found that EGFP–SIPP1 was no longer exclusively nuclear following the mutation (K31A/K32A/K34A/K35A) of the predicted NLS (Figure 8G). Nevertheless, EGFP–SIPP1-(45–641) and EGFP–SIPP1-K31A/K32A/K34A/K35A were still partially nuclear, indicating either that SIPP1 harbours at least one additional NLS or that SIPP1 can enter the nucleus by association with other proteins that are transported actively to the nucleus. Finally, we noted that SIPP1-V308A/F310A/V219A/F221A, which is mutated in both PP1-binding sites, has the same subcellular localization as wild-type SIPP1 (Figure 8H). The latter suggests that the association with PP1 does not play a role in the nuclear localization of SIPP1.

SIPP1 is a pre-mRNA splicing factor

Since SIPP1 is associated with the splicing factor compartments or speckles [19], which are believed to represent storage and/or assembly sites for splicing factors [28], we have explored whether SIPP1 is also recruited to the spliceosomes and has a role in pre-mRNA splicing. In Figure 9(A), it is shown that the splicing of a β-globin pre-mRNA fragment by a HeLa cell-splicing extract was nearly completely blocked by the addition of SIPP1-(180–372). The splicing intermediates of the first *trans*-esterification reaction (exon 1, lariat-exon 2) still accumulated, indicating that

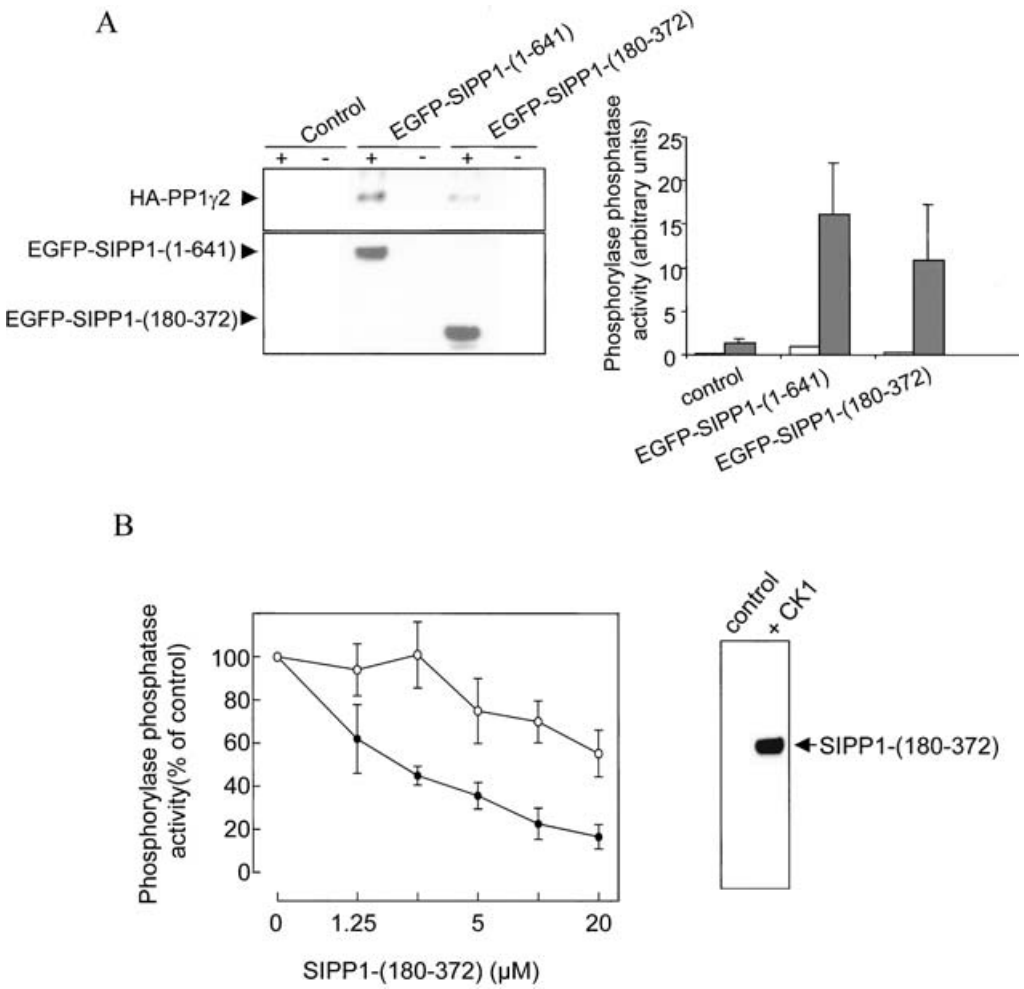

Figure 6 SIPP1 is an inhibitor of PP1

(**A**) COS-1 cells were transfected with both HA–PP1γ2 and either EGFP–SIPP1 or EGFP–SIPP1-(180–372). After lysis of the cells, SIPP1 was immunoprecipitated from the lysates with anti-EGFP antibodies. The immunoprecipitated EGFP–SIPP1 (fragment) and the co-immunoprecipitated PP1γ2 were detected by Western blot analysis (left-hand panel) with anti-EGFP and anti-HA antibodies respectively. The immunoprecipitates were obtained with (+) and without (−) primary anti-EGFP antibodies. PP1γ2 in the immunoprecipitates was also measured by the assay of phosphorylase phosphatase activities (right-hand panel) (means ± S.E.M. for three assays) before (open bars) and after trypsinolysis (closed bars). (**B**) Effect of GST–SIPP1-(180–372) on the phosphorylase phosphatase activity of PP1 (left-hand panel). The figure shows the effect of GST–SIPP1-(180–372) before (open circles) and after (closed circles) its phosphorylation by protein kinase CK1. The right-hand panel shows an autoradiogram of recombinant GST–SIPP1-(180–372) after a pre-incubation with Mg^{2+}, [γ^{32}P]ATP and protein kinase CK1 and subsequent SDS/PAGE. In the control condition no GST–SIPP1-(180–372) was added. The results are means ± S.E.M. for three different experiments.

SIPP1-(180–372) interferes with the second step of pre-mRNA splicing catalysis. PP1 has previously been shown to inhibit pre-mRNA splicing in nuclear extracts [29]. However, mutation of the PP1-binding sites of SIPP1-(180–372) did not interfere with its ability to block pre-mRNA splicing, indicating that this effect of SIPP1 cannot be accounted for by the targeting of splicing factors for dephosphorylation by PP1.

In further agreement with a role for SIPP1 as a splicing factor, we found that the immunoprecipitation of endogenous SIPP1 from HeLa cell-splicing extracts resulted in the co-precipitation of the pre-mRNA globin fragment, as well as the splicing intermediates and the splicing products (Figure 9B). This suggests strongly that SIPP1 is a component of functional spliceosomes. Interestingly, the addition of SIPP1-(180–372) did not interfere with the co-precipitation of pre-mRNA and SIPP1, indicating that the inhibition of splicing by this SIPP1 fragment cannot be accounted for by the displacement of full-length SIPP1 from the spliceosomes.

DISCUSSION

SIPP1 is a novel interactor of PP1

In the present study, we have shown, using two-hybrid analysis, GST pull-down assays and co-immunoprecipitations, that SIPP1 is an interactor of PP1 (Figures 1–6). The SIPP1–PP1 binding was also observed with purified components (Figures 2B, 3 and 6B), demonstrating that it is a direct interaction and is not mediated by a third component. In accordance with what is known for most other interactors of PP1, SIPP1 has multiple binding sites for PP1. A key interaction involves the binding of SIPP1 to the RVXF-binding channel of PP1, as confirmed by mutagenesis studies and by competition with established RVXF peptides (Figure 3). SIPP1 contains a canonical RVXF sequence (R^{217}KVGF^{221}) and a RVXF-like motif (L^{306}SVRF^{310}), since it lacks the mandatory basic residue at position 1 (or −1). Interestingly, our mutagenesis studies (Figure 3) suggest that both sequences are involved in the binding to PP1. It remains to be explored whether the RVXF-like

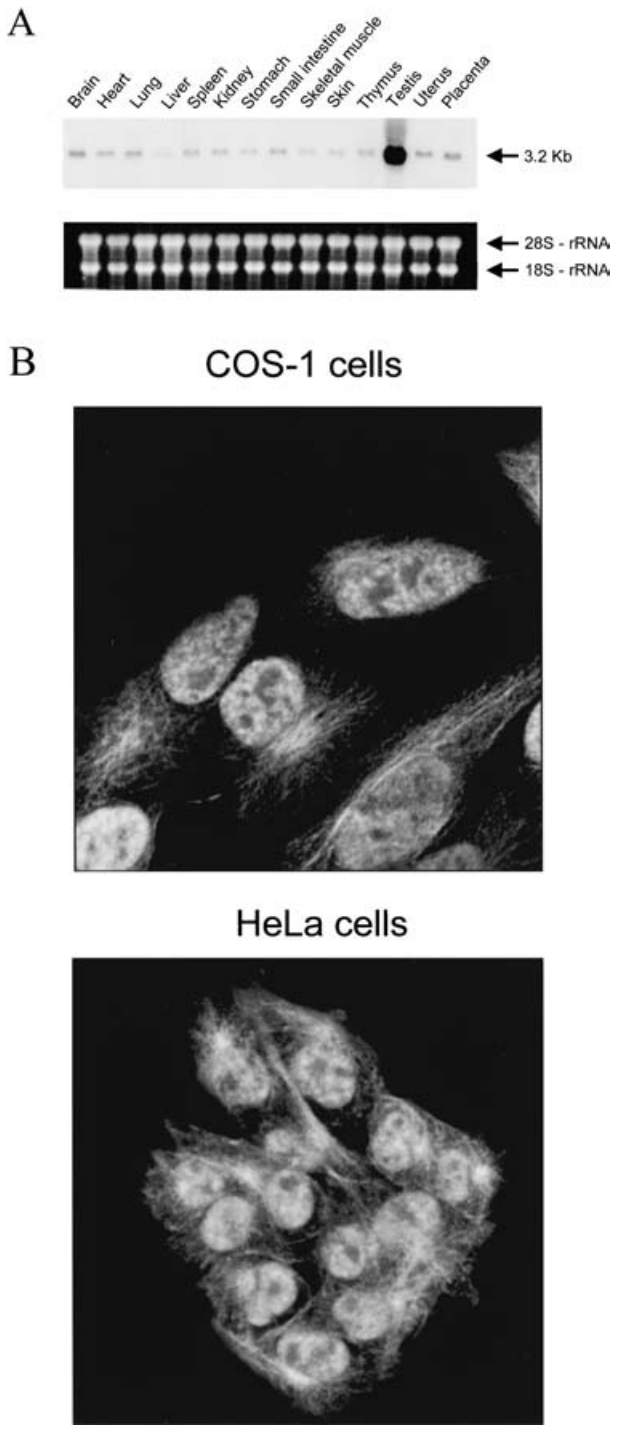

Figure 7 Tissue and subcellular distribution of SIPP1

(**A**) Northern blot analysis of adult mouse tissues. A blot with RNAs (20 μg/lane) from the indicated tissues was hybridized with a probe corresponding to nucleotides 292–514 of the SIPP1 cDNA. Also shown is an ethidium bromide staining of the blot illustrating an equal loading of the 18 S and 28 S rRNAs. (**B**) Subcellular distribution of endogenous SIPP1 in COS-1 and HeLa cells, as revealed by immunofluorescence analysis using anti-SIPP1 antibodies and FITC-labelled secondary antibodies.

motif actually also binds to the same hydrophobic groove as the canonical RVXF motif of SIPP1. The presence of multiple PP1-binding RVXF(-like) motifs in a single polypeptide is not unique and has also been suggested for the Aurora-A kinase [30].

PP1 that co-immunoprecipitated with EGFP–SIPP1 and EGFP–SIPP1-(180–372) from cell lysates was completely inactive (Figure 6). Recombinant SIPP1-(180–372), which encompasses the two established PP1-binding sites, was also inhibitory, albeit only at high concentrations. Phosphorylation by protein kinase CK1 increased the inhibitory potency of SIPP1-(180–372), but not enough to account for the complete inhibition of PP1 in the SIPP1 immunoprecipitates. Thus it remains possible that recombinant SIPP1-(180–372) lacks the proper conformation or post-translational modification for potent inhibition of PP1. It is also possible that the complete inhibition of PP1 in the SIPP1 immunoprecipitates is mediated by a third component. In this respect, it is important to note that PP1 has been shown to be present in complexes that contain multiple PP1-interacting proteins. For example, PP1 can form a heterotrimer with Inhibitor-1 and the growth arrest and DNA-damage-inducible protein GADD34 [31]. Both GADD34 and Inhibitor-1 contain an RVXF motif, but in the heterotrimeric complex, only GADD34 interacts with PP1 via an RVXF motif. Inhibitor-1 binds directly to GADD34 and only interacts with PP1 as a competitive inhibitor after phosphorylation.

Function of SIPP1 and associated PP1

Various lines of evidence indicate that SIPP1 is a pre-mRNA splicing factor. First, SIPP1 interacts with RNA [18,19] and with the polyglutamine-tract binding protein PQBP-1/Npw38, which also binds to the splicing factor U5-15 kDa protein, a component of U4/U6.U5 tri-snRNP (small nuclear ribonucleoprotein) [34,35]. Secondly, SIPP1 is targeted to the nuclear speckles (Figures 7B and 8, and [19]), which function as storage/assembly sites for splicing factors [28]. SIPP1 is also associated with the spliceosomes, the nuclear protein–RNA complexes that catalyse pre-mRNA splicing (Figure 9). SIPP1 co-precipitates with pre-mRNA splicing intermediates, as well as splicing products, indicating that it is associated with the spliceosomes throughout the splicing process. Interestingly, SIPP1 was also identified recently by MS as a component of affinity-purified spliceosomes [36]. In further agreement with a role for SIPP1 in pre-mRNA processing, we found that SIPP1-(180–372) blocks pre-mRNA splicing in nuclear extracts. This inhibition was independent of functional PP1-binding sites and could not be explained by a decreased targeting of endogenous SIPP1 to the spliceosomes (Figure 9). These data suggest that the splicing inhibition by SIPP1-(180–372) results from the titration of an as yet unidentified interactor of this SIPP1 fragment. SIPP1-(180–372) contains proline-rich and aspartic-rich regions (Figure 1), which may function as protein-interaction motifs.

An insight into the function of SIPP1 and associated PP1 is likely to come from a more detailed knowledge of the SIPP1 ligands. The C-terminal domain of SIPP1, which is required for the targeting to the speckles (Figure 8), harbours a proline-rich domain that has been shown to mediate binding to the WW domain of PQBP-1/Npw38BP [18]. Independently, Craggs et al. [19] reported that the proline-rich domains of SIPP1 also interact *in vitro* with some SH3 domains. It is not clear whether the affinity for SH3 domains is physiologically relevant or merely reflects the similar ligand specificity of SH3 domains and some WW-domain subtypes [38]. Interestingly, the WW domain of PQBP-1 has also been shown to bind to the C-terminal domain of the large subunit of RNA polymerase II and this interaction is improved by phosphorylation of this domain [39]. Recently, PP1 has been identified as one of the enzymes that dephosphorylates the C-terminal domain of RNA polymerase II [40]. By analogy, we

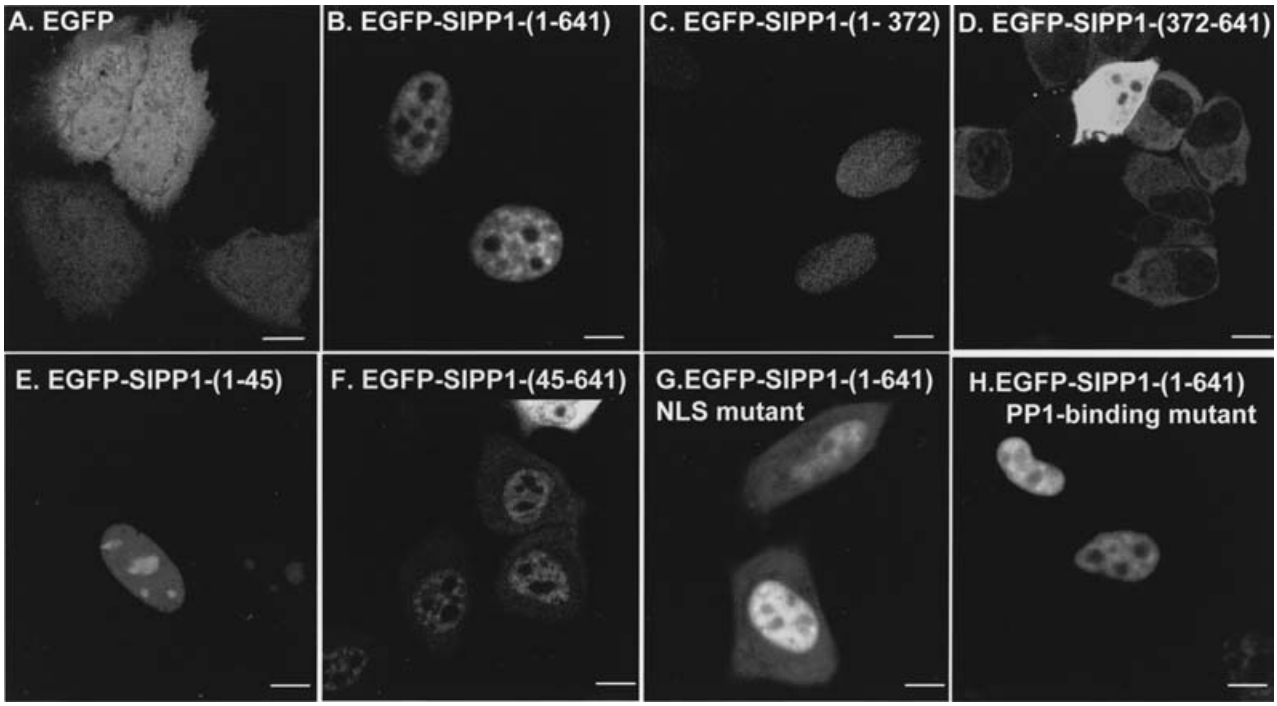

Figure 8 Determinants of the nuclear and subnuclear targeting of EGFP-SIPP1 in HeLa cells

EGFP, EGFP-tagged SIPP1 or the indicated EGFP-tagged SIPP1 fragments were transiently expressed in HeLa cells and their subcellular localization was analysed by confocal laser scanning microscopy. The Figure shows representative images of each transfection. The NLS mutant (panel G) refers to K31A/K32A/K34A/K35A. The PP1-binding mutant refers to V219A/F221A/V308A/F310A.

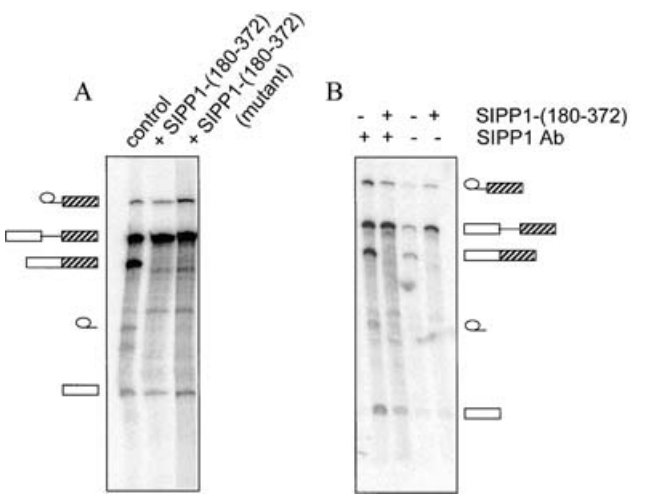

Figure 9 SIPP1 associates with spliceosomes and a SIPP1 fragment blocks pre-mRNA splicing in nuclear extracts

(**A**) Splicing of a radioactively labelled β-globin pre-mRNA fragment by HeLa cell nuclear extracts was carried out for 90 min at 30 °C in the absence (control) or presence of either 10 μM SIPP1-(180–372) or 10 μM SIPP1-(180–372)-V219A/F221A/V308A/F310A (mutant). The occurrence of splicing was evaluated by autoradiography after denaturing PAGE (9 %) of the phenol-extracted RNA. The splicing substrate and products are, from top to bottom, the lariat-exon 2, pre-mRNA, mRNA, the lariat and exon 1, and these RNA species are schematically identified at the left. (**B**) Co-immunoprecipitation of endogenous SIPP1 from the splicing extracts with exogenous ^{32}P-labelled β-globin pre-mRNA and its splicing products. The immunoprecipitations were performed in the absence or presence of 10 μM SIPP1-(180–372), which blocks pre-mRNA splicing (**A**).

speculate that the binding of the WW domain of PQBP-1 to SIPP1 is also enhanced by the phosphorylation of SIPP1 and that SIPP1-associated PP1 dephosphorylates SIPP1 and thereby decreases

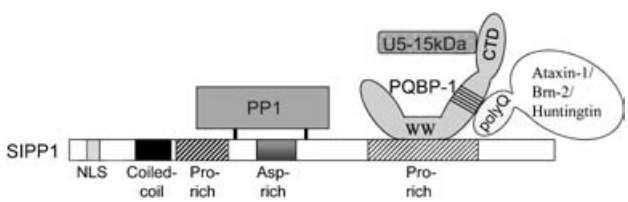

Figure 10 Interactors of SIPP1 and PQBP-1

CTD, C-terminal domain.

the SIPP1–PQBP-1 interaction. A phosphorylation-dependent interaction with splicing factors has also been established for NIPP1, another nuclear PP1-interactor. NIPP1 contains a Forkhead-associated domain that binds to phosphorylated forms of the splicing factors SAP155 and CDC5L [41,42].

In addition to a role in pre-mRNA splicing, PQBP-1 has also been implicated in transcriptional repression. The central domain of PQBP-1 contains di- and hepta-amino acid repeats that bind to the polyglutamine tracts of various proteins (Figure 10), including the transcription factor Brn-2, the Huntingtin protein and ataxin-1 [34,39]. These polyglutamine tracts are expanded in certain mutations that have been associated with neurodegenerative disorders known as triplet repeat disorders and the expanded tracts interact better with PQBP-1 [39]. The binding of ataxin to PQBP-1 also increased the binding of RNA polymerase II [39]. This reduces the level of RNA polymerase II phosphorylation and transcription. It will be interesting to investigate whether or not the binding of ligands to the central domain of PQBP-1 also affects the binding of SIPP1 to the WW domain.

This work was financially supported by the Spanish Ministerio de Ciencia y Cultura (PM 98-0150), by the Fund for Scientific Research-Flanders (Grant G.0374.01) and by

a Flemish Concerted Research Action. M. L. was the recipient of an EMBO short-term Fellowship (ASTF-94-2002). We thank Dr Amparo Cano for helping us to set up the yeast two-hybrid screening procedure. Dr K. Tatchell is acknowledged for the gift of the alanine-scanning mutants of Glc7 and Dr Stefaan Keppens for help with fluorescence microscopy. Nicole Sente provided expert technical assistance.

REFERENCES

1 Bollen, M. (2001) Combinatorial control of protein phosphatase-1. Trends Biochem. Sci. **26**, 426–431
2 Bollen, M. and Beullens, M. (2002) Signaling by protein phosphatases in the nucleus. Trends Cell Biol. **12**, 138–145
3 Ceulemans, H., Stalmans, W. and Bollen M. (2002) Regulator-driven functional diversification of protein phosphatase-1 in eukaryotic evolution. BioEssays **24**, 371–381
4 Cohen, P. T. W. (2002) Protein phosphatase 1 – targeted in many directions. J. Cell Sci. **115**, 241–256
5 Egloff, M.-P., Johnson, D. F., Moorhead, G., Cohen, P. T. W., Cohen, P. and Barford, D. (1997) Structural basis for the recognition of regulatory subunits by the catalytic subunit of protein phophatase 1. EMBO J. **16**, 1876–1887
6 Zhao, S. and Lee, E. Y. C. (1997) Targeting of the catalytic subunit of protein phosphatase-1 to the glycolytic enzyme phosphofructokinase. J. Biol. Chem. **272**, 28368–28372
7 Wakula, P., Beullens, M., Ceulemans, H., Stalmans, W. and Bollen, M. (2003) Degeneracy and function of the ubiquitous RVXF-motif that mediates binding to protein phosphatase-1. J. Biol. Chem. **278**, 18817–18823
8 Stralfors, P., Hiraga, A. and Cohen, P. (1985) The protein phosphatases involved in cellular regulation: purification and characterisation of the glycogen-bound form of protein phosphatase-1 from rabbit skeletal muscle. Eur. J. Biochem. **149**, 295–303
9 Beullens, M., Van Eynde, A., Stalmans, W. and Bollen, M. (1992) The isolation of novel inhibitory polypeptides of protein phosphatase 1 from bovine thymus nuclei. J. Biol. Chem. **267**, 16538–16544
10 Alessi, D., MacDougall, L. K., Sola, M. M., Ikebe, M. and Cohen, P. (1992) The control of protein phosphatase-1 by targetting subunits: the major myosin phosphatase in avian smooth muscle is a novel form of protein phosphatase-1. Eur. J. Biochem. **210**, 1023–1035
11 Campos, M., Fadden, P., Alms, G., Qian, Z. and Haystead, T. A. J. (1996) Identification of protein phosphatase-1-binding proteins by microcystin-biotin affinity chromatography. J. Biol. Chem. **271**, 28478–28484
12 Walsh, E. P., Lamont, D. J., Beattie, K. A. and Stark, M. J. (2002) Novel interactions of *Saccharomyces cerevisiae* type 1 protein phosphatase identified by single-step affinity purification and mass spectrometry. Biochemistry **41**, 2409–2420
13 Ceulemans, H., Vulsteke, V., De Maeyer, M., Tatchell, K., Stalmans, W. and Bollen, M. (2002) Binding of the concave surface of the Sds22 superhelix to the α4/α5/α6-triangle of protein phosphatase-1. J. Biol. Chem. **277**, 47331–47337
14 Helps, N. R., Barker, H. M., Elledge, S. J. and Cohen, P. T. W. (1995) Protein phosphatase 1 interacts with p53BP2, a protein which binds to the tumour suppressor p53. FEBS Lett. **377**, 295–300
15 Hartshorne, D. J. and Hirano, K. (1999) Interactions of protein phosphatase type 1, with a focus on myosin phosphatase. Mol. Cell. Biochem. **190**, 79–84
16 Ayllón, V., Cayla, X., García, A., Roncal, F., Fernández, R., Albar, J. P., Martínez-A., C. and Rebollo, A. J. (2001) Bcl-2 targets protein phosphatase 1α to Bad. J. Immunol. **166**, 7345–7352
17 Rudenko, A., Bennett, D. and Alphey, L. (2003) Trithorax interacts with type 1 serine/threonine protein phosphatase in *Drosophila*. EMBO Rep. **4**, 59–63
18 Komuro, A., Saeki, M. and Kato, S. (1999) Association of two nuclear proteins, Npw38 and NpwBP, via the interaction between the WW domain and a novel proline-rich motif containing glycine and arginine. J. Biol. Chem. **274**, 36513–36519
19 Craggs, G., Finan, P. M., Lawson, D., Wingfield, J., Perera, T., Gadher, S., Totty, N. F. and Kellie, S. (2001) A nuclear SH3 domain-binding protein that colocalizes with mRNA splicing factors and intermediate filament-containing perinuclear networks. J. Biol. Chem. **276**, 30552–30560
20 DeGuzman, A. and Lee, E. Y. C. (1988) Preparation of low-molecular-weight forms of rabbit muscle protein phosphatase. Methods Enzymol. **159**, 356–368
21 Baker, S. H., Frederick, D. L., Bloecher, A. and Tatchell, K. (1997) Alanine-scanning mutagenesis of protein phosphatase type 1 in the yeast *Saccharomyces cerevisiae*. Genetics **145**, 615–626
22 Louvet, O., Doignon, F. and Crouzet, M. (1997) Stable DNA-binding yeast vector allowing high-bait expression for use in the two-hybrid system. BioTechniques **23**, 816–818, 820
23 Crespo, P., Xu, N., Daniotti, J. L., Troppmair, J., Rapp, U. R. and Gutkind, J. S. (1994) Signaling through transforming G protein-coupled receptors in NIH 3T3 cells involves c-Raf activation: evidence for a protein kinase C-independent pathway J. Biol. Chem. **269**, 21103–21109
24 Beullens, M., Stalmans, W. and Bollen, M. (1998) The isolation of novel inhibitory polypeptides of protein phosphatase 1 from bovine thymus nuclei. Methods Mol. Biol. **93**, 145–155
25 Beullens, M. and Bollen, M. (2002) The protein phosphatase-1 regulator NIPP1 is also a splicing factor involved in a late step of spliceosome assembly. J. Biol. Chem. **277**, 19885–19860
26 Egloff, M.-P., Cohen, P. T. W., Reinemer, P. and Barford, D. (1995) Crystal structure of the catalytic subunit of human protein phosphatase 1 and its complex with tungstate. J. Mol. Biol. **254**, 942–959
27 Goldberg, J., Huang, H., Kwon, Y., Greengard, P., Nairn, A. C. and Kuriyan, J. (1995) Three-dimensional structure of the catalytic subunit of protein serine/threonine phosphatase-1. Nature (London) **376**, 745–753
28 Misteli, T. and Spector, D. L. (1997) Protein phosphorylation and the nuclear organization of pre-mRNA splicing. Trends Cell Biol. **7**, 135–138
29 Mermoud, J. E., Cohen, P. T. and Lamond, A. I. (1994) Regulation of mammalian spliceosome assembly by a protein phosphorylation mechanism. EMBO J. **13**, 5679–5688
30 Katayama, H., Zhou, H., Li, Q., Tatsuka, M. and Sen, S. (2001) Interaction and feedback regulation between STK15/BTAK/Aurora-A kinase and protein phosphatase 1 through mitotic cell division cycle. J. Biol. Chem. **276**, 46219–46224
31 Connor, J. H., Weiser, D. C., Li, S., Hallenbeck, J. M. and Shenolikar, S. (2001) Growth arrest and DNA damage-inducible protein GADD34 assembles a novel signaling complex containing protein phosphatase 1 and inhibitor 1. Mol. Cell. Biol. **21**, 6841–6850
32 Reference deleted
33 Reference deleted
34 Waragai, M., Junn, E., Kajikawa, M., Takeuchi, S., Kanzawa, I., Shibata, M., Mouradian, M. M. and Okazawa, H. (2000) PQBP-1/Npw38, a nuclear protein binding to the polyglutamine tract, interacts with U5–15kD/dim1p via the carboxyl-terminal domain. Biochem. Biophys. Res. Commun. **273**, 592–595
35 Zhang, Y.-Z., Lindblom, T., Chang, A., Sudol, M., Sluder, A. E. and Golemis, E. A. (2000) Evidence that dim1 associates with proteins involved in pre-mRNA splicing and delineation of residues essential for dim1 interactions with hnRNP F and Npw38/PQBP-1. Gene **257**, 33–43
36 Zhou, Z., Licklider, L. J., Gygi, S. P. and Reed, R. (2002) Comprehensive proteomic analysis of the human spliceosome. Nature (London) **419**, 182–185
37 Reference deleted
38 Macias, M. J., Wiesner, S. and Sudol, M. (2002) WW and SH3 domains, two different scaffolds to recognize proline-rich ligands. FEBS Lett. **513**, 30–37
39 Okazawa, H., Rich, T., Chang, A., Lin, X., Waragai, M., Kajikawa, M., Enokido, Y., Komuro, A., Kato, S., Shibata, M. et al. (2002) Interaction between mutant ataxin-1 and PQBP-1 affects transcription and cell death. Neuron **34**, 701–713
40 Washington, K., Ammosova, T., Beullens, M., Jerebtsova, M., Kumar, A., Bollen, M. and Nekai, S. (2002) Protein phosphatase-1 dephosphorylates the C-terminal domain of RNA polymerase-II. J. Biol. Chem. **277**, 40442–40448
41 Boudrez, A., Beullens, M., Groenen, P., Van Eynde, A., Vulsteke, V., Jagiello, I., Murray, M., Krainer, A. R., Stalmans, W. and Bollen, M. (2000) NIPP1-mediated interaction of protein phosphatase-1 with CDC5L, a regulator of pre-mRNA splicing and mitotic entry. J. Biol. Chem. **275**, 25411–25417
42 Boudrez, A., Beullens, M., Waelkens, E., Stalmans, W. and Bollen, M. (2002) Phosphorylation-dependent interaction between the splicing factors SAP155 and NIPP1. J. Biol. Chem. **277**, 31834–31841

Received 25 June 2003/10 November 2003; accepted 27 November 2003
Published as BJ Immediate Publication 1 December 2003, DOI 10.1042/BJ20030950